Redox Biology 46 (2021) 102077

Contents lists available at ScienceDirect

Redox Biology

journal homepage: www.elsevier.com/locate/redox

Oxidative stress following acute kidney injury causes disruption of lung cell cilia and their release into the bronchoaveolar lavage fluid and lung injury, which are exacerbated by *Idh2* deletion

Yong Kwon Han [a], Ji Su Kim [a], Gwan Beom Lee [a], Jae Hang Lim [b], Kwon Moo Park [a,*]

[a] Department of Anatomy, Cardiovascular Research Institute and BK21 Plus, School of Medicine, Kyungpook National University, 680 Gukchaebosang-ro, Junggu, Daegu, 41944, Republic of Korea
[b] Department of Microbiology, School of Medicine, Ihwa Woman's University, 25 Magokdong-ro 2-gil, Gangseo-gu, Seoul, 07804, Republic of Korea

ARTICLE INFO

Keywords:
Acute kidney injury
Cilia
Deciliation
Isocitrate dehydrogenase 2
Oxidative stress
Remote organ injury
Acute lung injury

ABSTRACT

Acute kidney injury (AKI) induces distant organ injury, which is a serious concern in patients with AKI. Recent studies have demonstrated that distant organ injury is associated with oxidative stress of organ and damage of cilium, an axoneme-based cellular organelle. However, the role of oxidative stress and cilia damage in AKI-induced lung injury remains to be defined. Here, we investigated whether AKI-induced lung injury is associated with mitochondrial oxidative stress and cilia disruption in lung cells. AKI was induced in isocitrate dehydrogenase 2 (*Idh2*, a mitochondrial antioxidant enzyme)-deleted ($Idh2^{-/-}$) and wild-type ($Idh2^{+/+}$) mice by kidney ischemia-reperfusion (IR). A group of mice were treated with Mito-TEMPO, a mitochondria-specific antioxidant. Kidney IR caused lung injuries, including alveolar septal thickening, alveolar damage, and neutrophil accumulation in the lung, and increased protein concentration and total cell number in bronchoalveolar lavage fluid (BALF). In addition, kidney IR caused fragmentation of lung epithelial cell cilia and the release of fragments into BALF. Kidney IR also increased the production of superoxide, lipid peroxidation, and mitochondrial and nuclei DNA oxidation in lungs and decreased IDH2 expression. Lung oxidative stress and injury relied on the degree of kidney injury. *Idh2* deletion exacerbated kidney IR-induced lung injuries. Treatment with Mito-TEMPO attenuated kidney IR-induced lung injuries, with greater attenuation in $Idh2^{-/-}$ than $Idh2^{+/+}$ mice. Our data demonstrate that AKI induces the disruption of cilia and damages cells via oxidative stress in lung epithelial cells, which leads to the release of disrupted ciliary fragments into BALF.

1. Introduction

Acute kidney injury (AKI) occurs in various clinical settings, including shock, sepsis, organ transplantation, and vascular surgery [1–3]. AKI causes damage to distant organs, including the lungs, liver, heart, and brain [4–9]. This distant organ injury following AKI is recognized as a major risk factor for poor outcomes [5,9]; therefore, appropriate treatment of distant organ injury is important to improve the outcome of patients with AKI. However, the precise mechanisms involved in AKI-related distant organ injury remain to be defined.

Cilia are centriole-derived projections from the cell surface that contain a microtubule-based cytoskeleton (axoneme), surrounded by a ciliary membrane. Cilia are characterized by their structure and motility and defined as either immotile cilia (primary cilia) or motile cilia. Primary cilia are solitary, non-motile, microtubule-based 9 + 0 axonemal antenna-like organelles that protrude from the cell membrane and transduce extracellular signals into the cell via the coordination of several signaling pathways [10–12]. Motile cilia, with a multiple, 9 + 2 axonemal structure, are mainly found in the respiratory tract and oviduct and function to transport materials [10,13]. Increasing evidence have demonstrated that defects in the formation and function of cilia are associated with diverse human diseases, including polycystic kidney diseases and primary ciliary dyskinesia [14–20]. Furthermore, recent studies have demonstrated that the disruption of cilia occurs under the influence of pathological conditions and that this disruption is involved in mediating cell injury and dysfunction [15–20].

* Corresponding author. Department of Anatomy, School of Medicine, Kyungpook National University, 680 Gukchaebosang-ro, Junggu, Daegu, 41944, Republic of Korea.
E-mail address: kmpark@knu.ac.kr (K.M. Park).

https://doi.org/10.1016/j.redox.2021.102077
Received 1 July 2021; Received in revised form 16 July 2021; Accepted 19 July 2021
Available online 21 July 2021

Accumulating evidence has demonstrated that kidney ischemia-reperfusion (IR), a cause of AKI, induces distant organ injury [6–8,21]. Distant organ injury is associated with inflammatory responses, changes in signaling pathways associated with cell death and survival, and oxidative stress [8,22–24]. Oxidative stress is directly linked to the dysfunction of cellular components, which can result in organ disorders, and recognized as one of the major causes of kidney IR-induced distant organ injury [21,25,26]. We have previously shown that kidney IR- and cisplatin-induced AKI alter the lengths of primary cilia in kidney epithelial cells via assembly, disassembly, and disruption (deciliation, shedding, or fragmentation) of cilia [17–19]. These processes are associated with reactive oxygen species (ROS) and oxidative stress, depending on the concentration of hydrogen peroxide and degree of oxidative stress; low H_2O_2 concentration induces the elongation of primary cilia length, whereas high H_2O_2 concentration induces disruption [17–20]. In addition, we found that disrupted primary cilia of injured kidney tubular epithelial cells are excreted into the urine and that this disruption and excretion can be prevented by antioxidant treatment [17–20]. Rodríguez-Ribera et al. also reported that reactive carbonyl compounds such as malondialdehyde, a product of oxidative stress, induce the loss of primary cilia in human kidney proximal tubule cells [27]. Therefore, we hypothesized that AKI-induced acute lung injury (ALI) and cell injury are associated with cilia and lung cell oxidative stress and that prevention of oxidative stress reduces AKI-induced lung injury. In the present study, we investigated whether kidney IR-induced AKI causes the disruption of cilia and cells of lungs, and if so, whether these disruptions are associated with oxidative stress. To this end, we employed pharmacological and genetic approaches, including the use of isocitrate dehydrogenase 2 (*Idh2*)-deleted mice. IDH2 is an enzyme localized in the mitochondria [28]. In the mitochondria, IDH2 catalyzes the oxidative decarboxylation of isocitrate to α-ketoglutarate, accompanied by the reduction of NADP to NADPH, which is a critical factor in the thioredoxin and glutathione antioxidant system [29–32]. In addition, we investigated whether the presence of ciliary proteins and fragments in bronchoalveolar lavage fluid (BALF) is indicative of lung injury. We report here, for the first time, that AKI causes disruption of lung cell cilia and their release into the BALF as well as lung injury, which is exacerbated by IDH2 deletion.

2. Materials & methods

Animal preparation. All experiments were conducted using 8–10-week-old male C57BL/6 mice (Koatech, Pyeongtaek, Gyeonggi-do, Korea), female *Idh2* gene-deleted (*Idh2*$^{-/-}$) mice, and wild-type (*Idh2*$^{+/+}$) mice [28]. The mice were allowed free access to water and standard mouse chow. The animal study was approved by the Institutional Animal Care and Use Committee of Kyungpook National University, Republic of Korea. To induce bilateral renal ischemia, the kidneys were exposed through flank incisions under anesthetization with pentobarbital sodium (60 mg/kg BW), and then, the pedicles of the kidneys were completely clamped for 35 min using micro aneurysm clamps. The same procedure, exclusive of kidney pedicle clamping, was performed in the sham operation Body temperature was maintained at 36.5°C-37 °C throughout surgical procedures using a temperature-controlled heating device (FHC, Bowdoin, ME, USA). Some mice were administered 2-(2,2,6,6-Tetramethylpiperidin-1-oxyl-4-ylamino)-2-oxoethyl) triphenylphosphonium chloride (Mito--TEMPO, 0.7 mg/kg BW; Sigma, St. Louis, MO, USA) at either 17 and 1 h before operation (pretreatment) or 6 h after operation (post-treatment).

At the end of the experiments, the lung and kidney tissues were snap-frozen in liquid nitrogen or perfusion fixed with PLP (4 % paraformaldehyde, 75 mM L-lysine, 10 mM sodium periodate; Sigma) solution for biochemical and histological studies, respectively. Frozen tissues were stored at −70 °C until required.

Collection of BALF. BALF was collected after euthanizing the mice by overdose injection of pentobarbital sodium. Lung leakages were evaluated by determining the protein concentration and cell number in the BALF. To collect BALF, the bronchus of the left lung was completely clamped using micro aneurysm clamps. A needle was inserted into the trachea and 0.8 ml cold phosphate buffered saline (PBS) was slowly injected into right lung lobes. BALF was collected by retracting the piston of the syringe once. Total cell number and protein concentration in BALF were analyzed immediately using a hematocytometer and BCA assay kit (Thermo Fisher Scientific, Waltham, Massachusetts, USA), respectively. BALF was kept at −70 °C until required for western blotting analysis.

Kidney function. Blood was collected from mice using a heparinized syringe. The concentration of blood urea nitrogen (BUN) in plasma was determined using a Vitros 250 Chemistry Analyzer (Johnson & Johnson, New Brunswick, NJ, USA).

Periodic acid-Schiff (PAS) and hematoxylin and eosin (H&E) staining. PLP-fixed kidney and lung tissues were paraffin-embedded, cut into 3-μm thick sections using a microtome (Leica, Bensheim, Germany), and mounted on glass slides. Kidney and lung sections were stained with PAS and H&E. The kidney damage score was evaluated blindly by investigators as described previously [3,19].

Western blot analysis. Western blotting was performed as previously described [3]. The antibodies used for western blotting were as follows: anti-4-hydroxynonenal (4-HNE; Abcam, Cambridge, MA, USA), anti-α-tubulin (Santa Cruz, CA, USA), anti-acetylated α-tubulin (ac-α-tubulin, Sigma), anti-manganese-dependent superoxide dismutase (MnSOD; Calbiochem, San Diego, CA, USA), anti-catalase (Fitzgerald, Concord, MA, USA), anti-ADP-ribosylation factor-like protein 13B (Arl13B, Proteintech, Chicago, IL, USA), anti-isocitrate dehydrogenase 2 (IDH2; Santa Cruz), anti-optic atrophy 1 (Opa1; BD Bioscience, San Diego, CA), anti-fission 1 (Fis1; Sigma), anti-dynamin related protein 1 (Drp1; Cell Signaling Technology, Danvers, MA, USA), and anti-glyceraldehyde 3-phosphate dehydrogenase (GAPDH; NOVUS, Littleton, CO, USA).

Immunofluorescent staining. After deparaffinization, sections were incubated in PBS containing 0.2 % Triton X-100 (Sigma) for 1 min and then washed in PBS for 10 min. To expose the antigen epitope, sections were boiled in 10 mM sodium citrate buffer (pH 6.0) for 10 min, cooled for 20 min, and then washed thrice with PBS for 5 min on each wash. The sections were blocked with 3 % bovine serum albumin in PBS (blocking buffer) for 30 min and then incubated with anti-Arl13b antibody at 4 °C overnight. After washing, the sections were incubated with FITC-conjugated goat anti-rabbit IgG (Vector Laboratories, Burlingame, CA, USA) for 60 min and then washed 3 times with PBS for 5 min each. Cell nuclei were stained using 4′-6-diamidino-2-phenylindole (DAPI; Sigma).

To stain Arl13B of BALFs, 10 μl of BALF was put on a glass slide and fixed with PLP solution. Fixed BALF on slides were used for immunofluorescent staining using the anti-Arl13b antibody as described above.

Immunohistochemical staining. After deparaffinization, sections were incubated in PBS containing 0.2 % Triton X-100 (Sigma) for 1 min and washed in PBS for 10 min. To expose the antigen epitope, sections were boiled in 10 mM sodium citrate buffer (pH 6.0) for 10 min, cooled for 20 min, and then washed 3 times with PBS for 5 min each. To remove the endogenous peroxidase activity, the tissue slide was reacted at room temperature for 30 min using 3 % hydrogen peroxide containing methanol and then blocked with blocking buffer for 30 min. Following blocking, the slide was incubated with anti-8-hydroxy-2′-deoxyguanosine (8-OHdG; Abcam, Cambridge, MA, USA) or anti-4-HNE antibody diluted in blocking buffer at 4 °C overnight. After washing, sections were incubated with HRP-conjugated goat anti-mouse IgG (Vector Laboratories) for 60 min and then washed three times with PBS for 5 min each. Subsequently, the slides were incubated with 3, 3′-diaminobenzidine (DAB; Vector Laboratories) solution to develop color and then counter-stained with hematoxylin. The sections were observed under a Leica microscope (Leica, Wetzlar, Germany).

Measurement of superoxide in lung tissue. Superoxide levels were

measured using dihydroethidium (DHE; Sigma) as described previously [33,34]. Briefly, 10 μM DHE in 1 ml of pre-warmed (37 °C) PBS was added to a 96-well plate containing 20 μl of lung tissue lysate. The plate was read every 10 min for a total of 30 min at excitation/emission filters of 530 nm/620 nm.

Measurement of IL-6. IL-6 levels in plasma and BALF were determined via ELISA assay using ELISA assay kit according to the manufacturer's instructions (BD Bioscience).

Statistics. All data were analyzed using GraphPad Prism 7 software (San Diego, CA, USA). The results are expressed as the mean ± standard error of the mean (SEM). Statistical analysis was performed using Student's t-test and one-way analysis of variance with Tukey's post hoc procedure. Differences were considered statistically significant when p-values were <0.05.

3. Results

1. Kidney IR causes lung injury. As expected, significant morphological damage to the kidneys (Fig. 1A and B) and increases in plasma BUN (Fig. 1C) were observed 4 and 24 h after 35 min of bilateral kidney ischemia. In the lung, an increase in neutrophils and alveolar wall thickening were observed 4 and 24 h after kidney ischemia (Fig. 1D). In addition, the increase in the expression of lymphocyte antigen 6 complex locus G6D (Ly6G, a marker for monocytes, granulocytes, and neutrophils) in lung tissue was observed in a reperfusion time-dependent manner (Fig. 1E and F). Interleukin-6 (IL-6) concentration in plasma increased after kidney IR, peaking at 4 h after ischemia (Fig. 1G). The IL-6 and protein concentrations as well as total cell number in BALF gradually increased at 4 and 24 h after kidney ischemia (Fig. 1H–J). The survival rate at 24 h after 35 min of kidney IR was approximately 92 % (data not shown).

When kidney ischemic time was extended to 45 min, post-ischemic increases in BUN concentration in plasma and total protein concentration and cell number in BALF were greater than those after 35 min of ischemia (Fig. 1K–M). These data indicate that lung injury induced by kidney IR injury relies on the degree of kidney injury.

2. Kidney IR causes disruption of cilia of lung epithelial cells and these fragments are released into BALF. Lung tissue sections and BALF-loaded slides were immunostained with anti-ADP-ribosylation factor-like protein 13B (Arl13B, a marker of cilia) antibody. Arl13B positive signals were observed on the luminal part of the alveoli and the terminal bronchioles of the lung (Fig. 2A). Loss of Arl13B-positive signal was observed in the lung of kidney IR-subjected mice (Fig. 2A). This loss of Arl13B-positive signal gradually increased after kidney ischemia over time (Fig. 2A). In BALF, various lengths of Arl13B-positive particles were observed after kidney ischemia, and the number of Arl13B-positive particles in BALF gradually increased over time after ischemia (Fig. 2B and C). The expression of Arl13B, acetylated α-tubulin (ac-α-tubulin, an

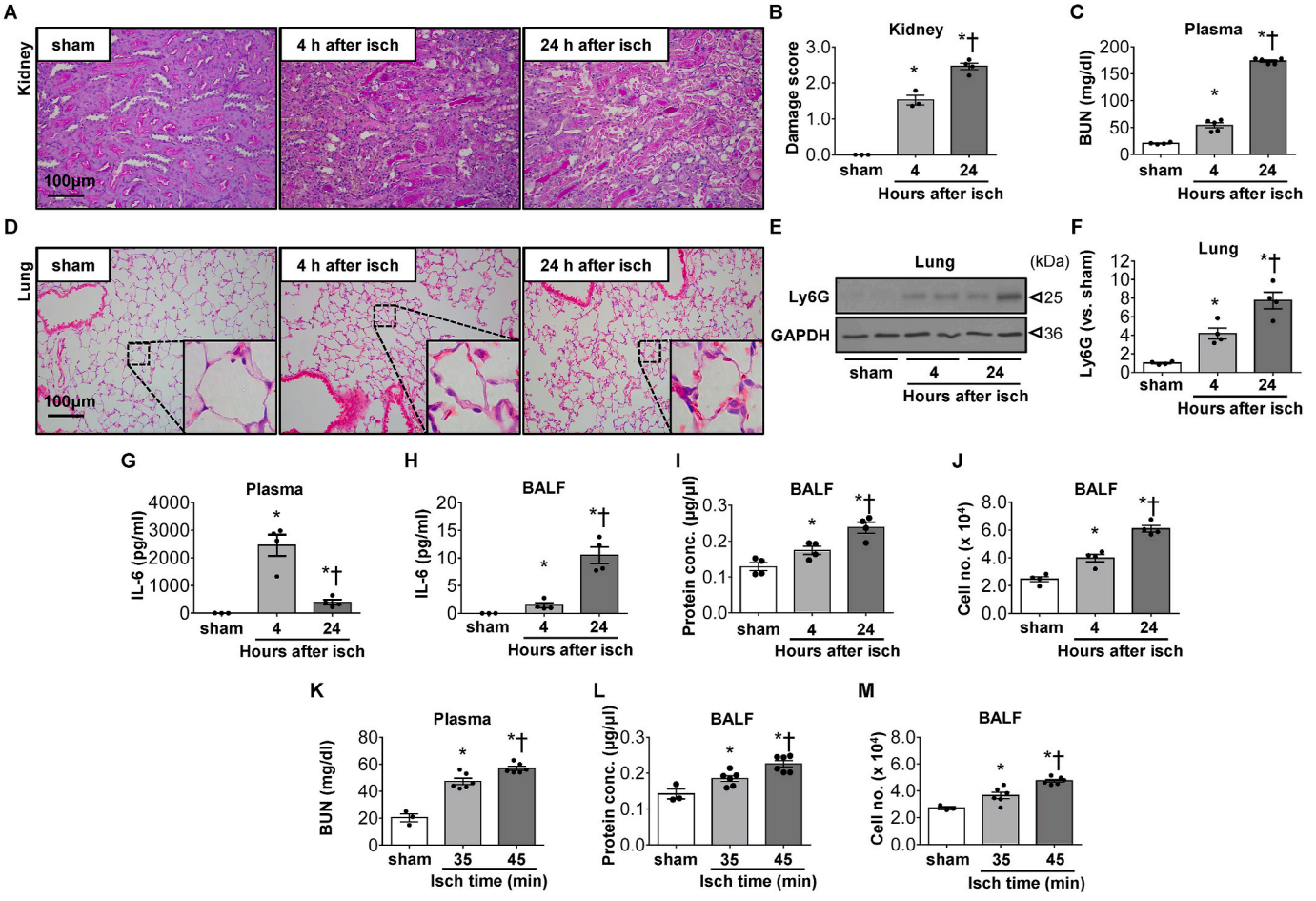

Fig. 1. Histological and functional damage of the lung after kidney IR. C57BL/6 male mice were subjected to 35 (A–M) and 45 (K–M) min of bilateral renal ischemia or sham operation. Kidney, lung, blood, and BALF were collected 4 and 24 h after operation. BALF was collected as described in the Materials and Methods. (A–J) Mice were sacrificed either 4 or 24 h after 35 min of ischemia. (A, B) Kidney sections (3 μm) were stained with PAS, and kidney tubular damage was scored. (C, K) BUN concentrations were measured in plasma. (D) Lung sections (3 μm) were stained with H&E. (E, F) Ly6G expression in lung tissue was analyzed by western blotting. GAPDH was used as a loading control. The densities of the bands were measured using the ImageJ software. (G, H) The IL-6 concentration was measured in plasma and BALF. (I, J, L, M) The protein concentration and total cell number were measured in BALF. (K–M) Mice were sacrificed 4 h after either 35 or 45 min of ischemia. Results are expressed as the means ± SEM (n = 3–6). *p < 0.05 vs. sham. †p < 0.05 vs. 4 h after ischemia or ischemia for 35 min.

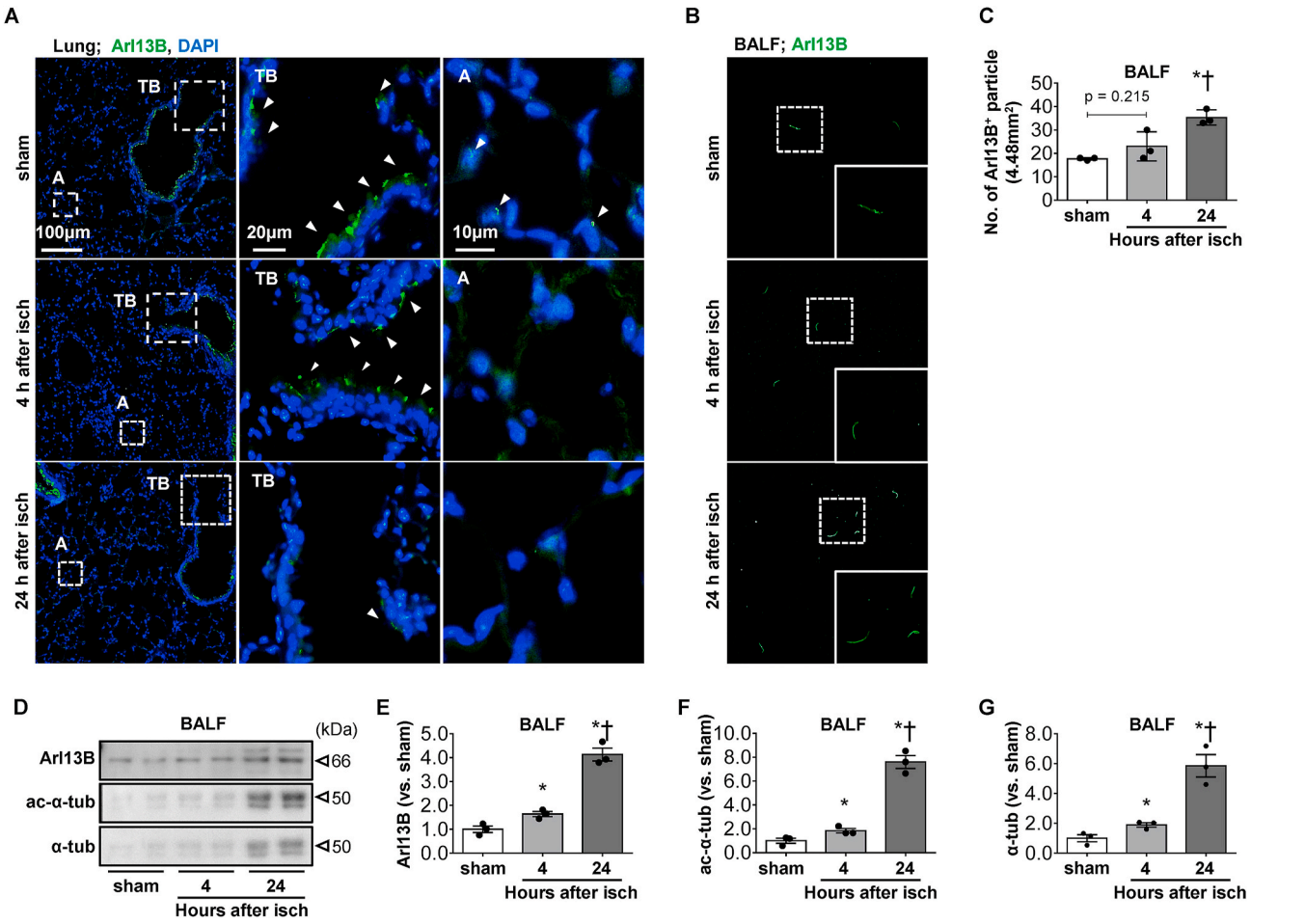

Fig. 2. Disruption in lung cell cilia and their fragments and proteins released into BALF after kidney IR. C57BL/6 male mice were subjected to either 35 min of bilateral renal ischemia or sham operation Lung tissue and BALF were collected 4 and 24 h after operation as described in the Materials and Methods. (A) Lung sections (5 μm) were subjected to immunofluorescent staining using anti-Arl13B antibody; green indicates Arl13B-positive. DAPI stain (4′,6-diamidino-2-phenylindole; blue) was used to visualize the nuclei of cells. Arrowheads indicate cilia. (B) BALF (10 μl) was put on a glass slide which was immunofluorescent-stained using anti-Arl13B antibody; green indicates Arl13B-positive (n = 3). (C) The number of Arl13B-positive particles was counted under a fluorescence microscope (n = 3). (D–G) Arl13B, acetylated-α-tubulin (ac-α-tub), and α-tubulin (α-tub) expressions in BALF were analyzed by western blotting. The densities of the bands were measured using the ImageJ software. Results are expressed as the means ± SEM (n = 3). *p < 0.05 vs. sham. †p < 0.05 vs. 4 h after ischemia. A: Alveoli, TB: Tubule. (For interpretation of the references to color in this figure legend, the reader is referred to the Web version of this article.)

acetylated form of α-tubulin, and widely used as a primary cilia marker), and α-tubulin (a major microtubule comprising protein) in BALF increased after kidney ischemia in a reperfusion–time-dependent manner (Fig. 2D–G). These results indicate that kidney IR causes disruption of cilia in lung epithelial cells, and these disrupted cilia fragments are released into BALF.

3. Kidney IR increases the levels of superoxide and oxidative stress in both lung tissue and BALF. Kidney IR increased the superoxide level in lung tissue (Fig. 3A), whereas it reduced the expression of IDH2 (Fig. 3B and C), but not MnSOD and catalase (Fig. 3B, D, E). These findings indicate that kidney IR-induced lung injury is associated with increases in ROS levels and oxidative stress in lungs. In support of this, the level of 4-hydroxynonenal (4-HNE), a product of lipid peroxidation, in the lung tissue significantly increased 4 and 24 h after kidney ischemia (Fig. 3F–I). 4-HNE was observed in almost all areas in lung tissue, including the alveoli and bronchioles (Fig. 3H and I). Furthermore, the expression of 8-hydroxy-2′-deoxyguanosine (8-OhdG), a well-known marker of DNA oxidation as an oxidized derivative of deoxyguanosine, increased in both the cytosol and nuclei in pulmonary epithelial cells after kidney ischemia (Fig. 3J and K). In BALF, 4-HNE expression also increased after kidney ischemia in a reperfusion–time-dependent manner (Fig. 3L, M). Furthermore, when kidney ischemic time was extended to 45 min, post-ischemic increase in 4-HNE expression in the lungs was greater than that after 35 min of kidney ischemia (Fig. 3N, O). These results indicate that both mitochondrial DNA and nuclear DNA are oxidatively injured by increased ROS formation and impairments in removal systems, suggesting that the damage to pulmonary epithelial cell cilia is associated with oxidative stress.

In cells, mitochondria. a major ROS-producing intracellular organelle, normally undergo fusion and fission to adapt to physiological and pathological conditions. Impairment in these fusion and fission processes can induce cell dysfunction and damage [36]. Previous studies have demonstrated that oxidative stress impairs the normal dynamics of mitochondrial fusion and fission, resulting in mitochondrial dysfunction and cell injury [32,36–38]. We sought to evaluate the mitochondrial dynamics by determining mitochondrial fission- and fusion-regulating protein expressions. The expressions of Fis1 and Drp1, which regulate mitochondrial fission, were significantly increased in the lungs of mice with kidney ischemia (Fig. 4A–C). However, the expression of OPA1, which regulates mitochondrial fusion, was not significantly altered by kidney IR (Fig. 4A, D). These data indicate that the balance of mitochondrial fusion and fission in lung cells is disrupted as a result of AKI.

4. Mitochondria-specific antioxidant treatment reduces kidney IR-induced lung injury and lung cilia disruption. To confirm the role

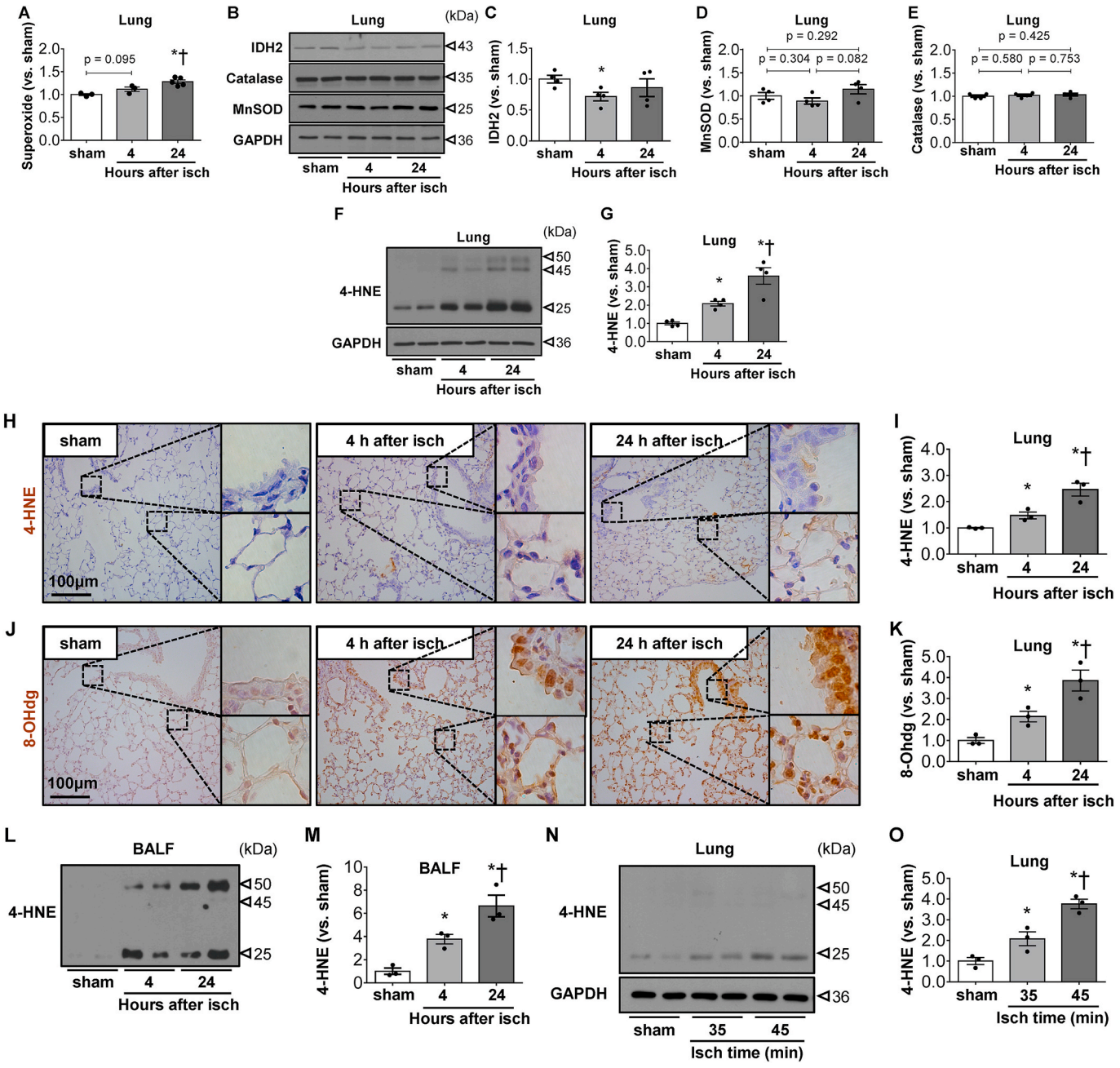

Fig. 3. Oxidative stress in lung tissue after kidney IR. C57BL/6 male mice were subjected to 35 (A–O) and 45 (N, O) min of bilateral renal ischemia or sham operation. Lung and kidney were harvested 4 and 24 h after either 35 min or 45 min of ischemia. (A–M) Mice were sacrificed either 4 or 24 h after 35 min of ischemia. (A) The superoxide level in the lung tissue was measured as described in the Materials and Methods (n = 3–5). (B–E) IDH2, catalase, and MnSOD expression in the lung tissue were analyzed by western blotting (n = 4). GAPDH was used as the loading control. (C–E) The densities of the bands were measured using ImageJ software. (F, G) 4-HNE expression in lung was analyzed by western blotting, and the band density was measured using ImageJ (n = 4). (H–K) Lung sections (3 μm) were immunohistochemically stained using anti-4-HNE and 8-OHdG antibodies and counter-stained using hematoxylin; brown indicates 4-HNE- and 8-OHdG-positive (n = 3). (I, K) The intensities of 4-HNE- and 8-OHdG-positive signals were measured using the i-Solution program (n = 3). (L, M) 4-HNE expression in BALF was analyzed by western blotting, and the band density was measured using ImageJ (n = 3). (N, O) Mice were sacrificed 4 h after either 35 min or 45 min of ischemia. 4-HNE expression in lung was analyzed by western blotting, and the band density was measured using ImageJ (n = 3). Results are expressed as the means ± SEM (n = 3–5). *p < 0.05 vs. sham. †p < 0.05 vs. 4 h after ischemia or 35 min of ischemia. (For interpretation of the references to color in this figure legend, the reader is referred to the Web version of this article.)

of mitochondrial oxidative stress on kidney IR-induced lung injury and lung epithelial cell cilia disruption, we tested whether pretreatment (Fig. 5A–I) or post-treatment (Fig. 5J–L) with Mito-TEMPO, a mitochondria-specific antioxidant, inhibits kidney IR-induced oxidative stress, IL-6 production, and deciliation in the lungs of C57BL/6 male mice. Pretreatment (Fig. 5A–I), but not post-treatment (Fig. 5J–L), with Mito-TEMPO significantly inhibited increases in BUN and IL-6 concentrations in plasma (Fig. 5A and B) as well as IL-6 concentration, total protein concentration, and total cell number in BALF (Fig, 5C-E). The expressions of Arl13B, ac-α-tubulin, and α-tubulin in the BALF of Mito-TEMPO-pre-treated mice were less than those in vehicle-treated mice (Fig. 5F–I). In this study, a 6-h post-treatment did not protect the lungs against kidney IR (Fig. 5J–L). These results indicate that early ROS production, its accumulation, and oxidative stress may importantly

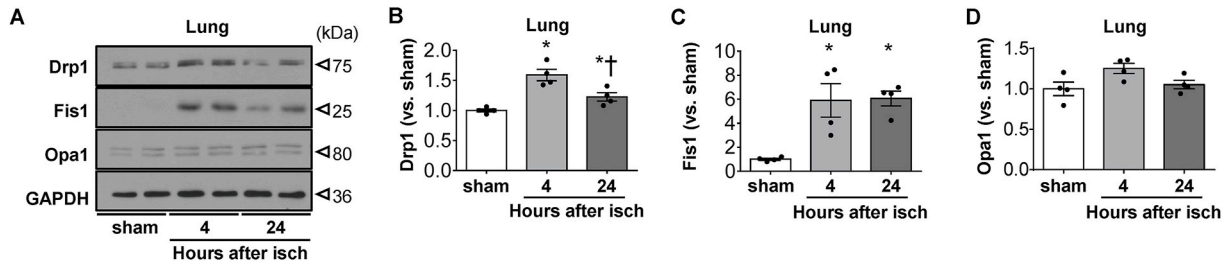

Fig. 4. Change in mitochondrial dynamics in the lung after kidney IR. C57BL/6 male mice were subjected to either 35 min of bilateral renal ischemia or sham operation. The lungs were harvested 4 and 24 h after ischemia. (A–D) Drp1, Fis1, and OPA1 expressions in lung tissues were analyzed by western blotting. GAPDH was used as the loading control. The densities of the bands were measured using the ImageJ software. Results are expressed as the means ± SEM (n = 4). *p < 0.05 vs. sham. †p < 0.05 vs. 4 h after ischemia.

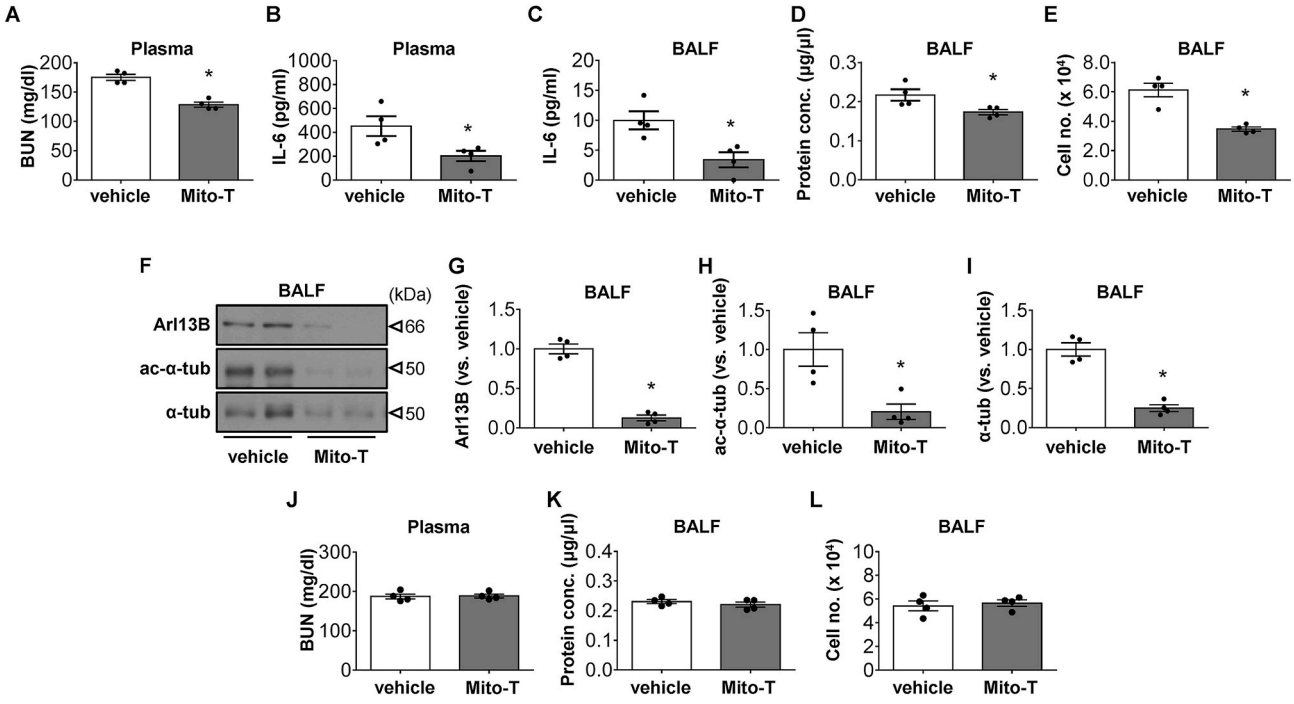

Fig. 5. Prevention of kidney IR-induced lung injury and cilia disruption by Mito-TEMPO, a mitochondria-targeted antioxidant. C57BL/6 male mice were subjected to 35 min of bilateral renal ischemia. Some mice were administered with Mito-TEMPO (Mito-T, 0.7 mg/kg BW, i.p.) either 17 and 1 h before ischemia, twice, (A–I) or 6 h after ischemia (J–L). Lung, BALF, and blood were harvested 24 h after ischemia. (A, J) The BUN concentration in plasma was measured. (B, C) IL-6 concentrations in plasma and BALF were measured using the ELISA assay kit. (D, E, K, L) The protein concentration and cell number in BALF were measured. (F–I) Arl13B, acetylated-α-tubulin (ac-α-tub), and α-tubulin (α-tub) expressions in BALF were analyzed by western blotting. The densities of the bands were measured using the ImageJ software. Results are expressed as the means ± SEM (n = 4). *p < 0.05 vs. vehicle.

contribute to AKI-induced lung injury.

Superoxide levels and 4-HNE expression in lung tissue (Fig. 6A–C) and in BALF (Fig. 6D and E) were less in Mito-TEMPO-pretreated mice than in vehicle-treated mice. These results indicate that kidney IR-induced lung injury and lung epithelial cell deciliation are associated with mitochondrial oxidative stress.

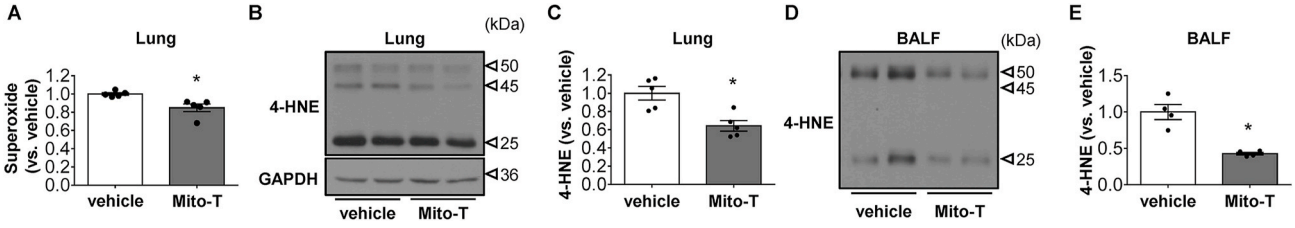

Fig. 6. Prevention of kidney IR-induced lung oxidative stress by Mito-TEMPO. C57BL/6 male mice were subjected to 35 min of bilateral renal ischemia. Some mice were administered Mito-TEMPO (Mito-T, 0.7 mg/kg BW, i.p.) 17 and 1 h before ischemia, twice. The lungs, BALF, and blood were obtained 24 h after ischemia. (A) Superoxide levels in lung tissue were measured (n = 5). (B–E) 4-HNE expression in the lung tissues (n = 5) (B, C) and BALF (n = 4) (D, E) were analyzed by western blotting. GAPDH was used as the loading control. The densities of the bands were measured using the ImageJ software. Results are expressed as the means ± SEM (n = 4–5). *p < 0.05 vs. vehicle.

5. *Idh2* deletion aggravates kidney IR-induced lung injury. Lastly, we investigated the role of IDH2 on kidney IR-induced lung injury. To define the role of IDH2 on lung oxidative stress and lung injury under conditions of no or minimal differences of kidney injury, we induced 35 min of kidney ischemia followed by 4 h of reperfusion in female *Idh2*$^{-/-}$ and *Idh2*$^{+/+}$ mice based on two points; 1) female mice are less susceptible to kidney IR injury and 4 h reperfusion causes less severe kidney injury than 24 h reperfusion [3,39,40]. As expected, 35 min of ischemia and 4 h reperfusion increased BUN concentrations in both *Idh2*$^{-/-}$ and *Idh2*$^{+/+}$ mice without significant difference in BUN between *Idh2*$^{-/-}$ and *Idh2*$^{+/+}$ mice (Fig. 7A). However, lung injury including increased neutrophil infiltration and alveolar septal thickening-was greater in *Idh2*$^{-/-}$ mice than *Idh2*$^{+/+}$ mice (Fig. 7B). Consistent with histological damage, approximately 58.5 % protein concentration and 37.8 % total cell number in BALF of *Idh2*$^{-/-}$ mice were higher than those in BALF of *Idh2*$^{+/+}$ mice (Fig. 7C and D). No significant differences in BUN and lung injury between *Idh2*$^{-/-}$ mice and *Idh2*$^{+/+}$ mice were observed after sham operation (Fig. 7A–D). These results indicate that the deficiency of the IDH2 gene, a mitochondrial antioxidant enzyme, worsens kidney IR-induced lung injury.

To further confirm the role of IDH2 and mitochondrial oxidative stress on kidney IR-induced lung injury, we evaluated whether Mito-TEMPO inhibits the increase of protein concentration and cell number in BALF after kidney IR. Mito-TEMPO treatment prevented the increase in protein concentration and total cell number after kidney IR in both *Idh2*$^{-/-}$ mice and *Idh2*$^{+/+}$ mice. This prevention was greater in *Idh2*$^{-/-}$ mice than in *Idh2*$^{+/+}$ mice (approximately 32.2 % in *Idh2*$^{+/+}$ and 38.6% in *Idh2*$^{-/-}$ in protein concentration in BALF and 8.4 % in *Idh2*$^{+/+}$ and 35.4 % in *Idh2*$^{-/-}$ in total cell number in BALF) (Fig. 7C and D). Mito-TEMPO slightly reduced BUN levels in both mice, but this was not

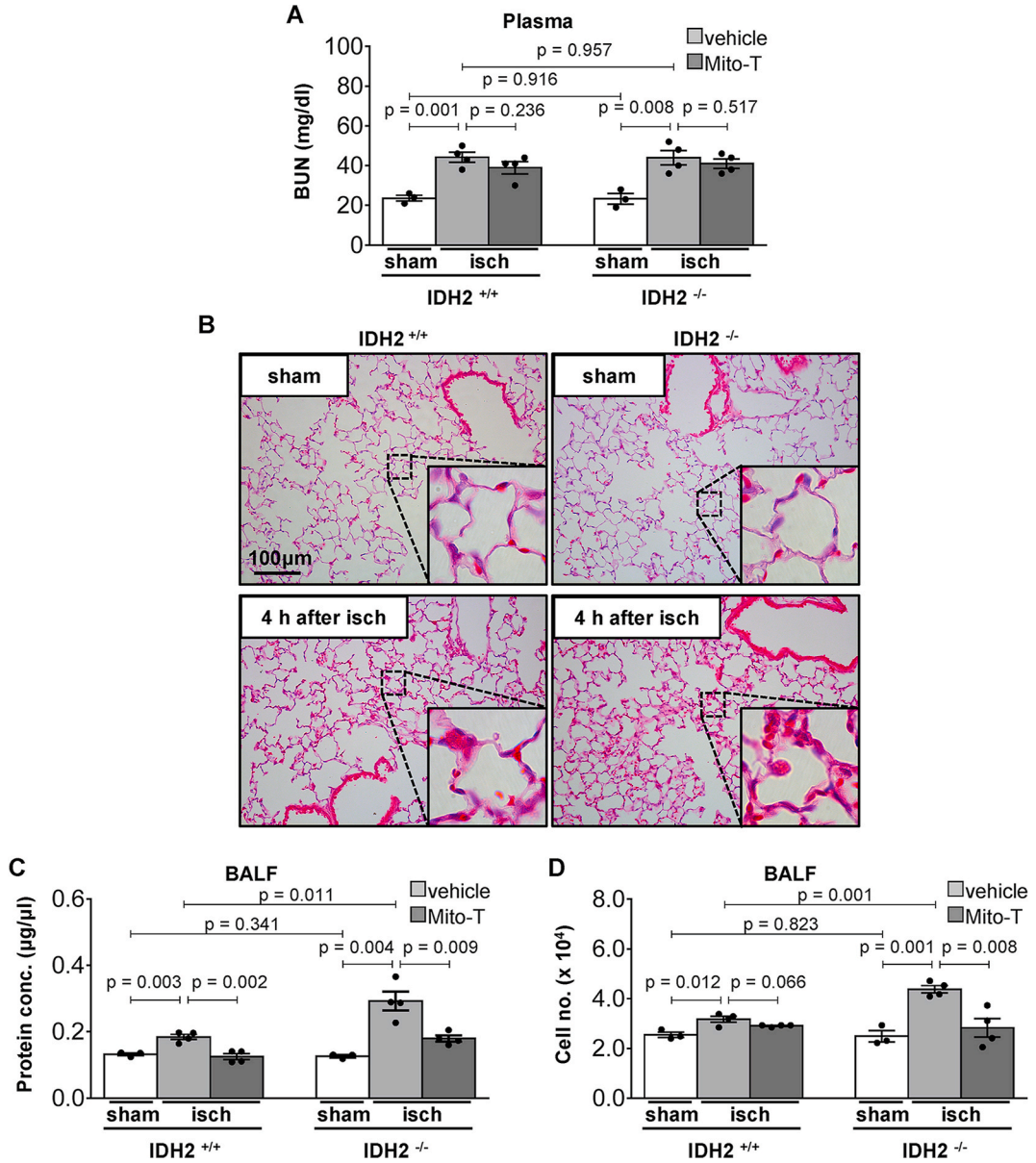

Fig. 7. Greater lung injury after kidney IR in *Idh2*$^{-/-}$ mice than in *Idh2*$^{+/+}$ mice and greater prevention of kidney IR-induced lung injury by Mito-TEMPO in *Idh2*$^{-/-}$ mice than in *Idh2*$^{+/+}$ mice. Female *Idh2*-deleted (*Idh2*$^{-/-}$) and wild-type (*Idh2*$^{+/+}$) littermates were subjected to 35 min of bilateral renal ischemia. Some mice were administered Mito-TEMPO (Mito-T, 0.7 mg/kg BW, i.p.) 17 and 1 h before ischemia, twice. Lung, BALF, and blood were collected 4 h after ischemia. (A) The BUN in plasma was measured as described in the Materials and Methods (n = 4). (B) Perfusion fixed lung tissues were cut into 3-μm thick sections, which were then subjected to H&E staining (n = 3). (C, D) The protein concentration and total cell number in BALF were measured as described in the Materials and Methods (n = 4). Results are expressed as the means ± SEM (n = 3–4).

statistically significant (Fig. 7A). These results indicate that IDH2 plays an important role in kidney IR-induced lung injury.

Kidney IR significantly increased 4-HNE expression in lungs in both *Idh2*$^{-/-}$ and *Idh2*$^{+/+}$ mice 4 h after kidney ischemia, and this increase were greater in *Idh2*$^{-/-}$ mice than in *Idh2*$^{+/+}$ mice ($p < 0.001$) (Fig. 8A and B). Mito-TEMPO prevented the increase in 4-HNE expression in both mice (37.5 % in *Idh2*$^{+/+}$ and 28.4 % in *Idh2*$^{-/-}$) (Fig. 8C and D). There were no significant differences in 4-HNE expression between sham-operated *Idh2*$^{+/+}$ and *Idh2*$^{-/-}$ mice (Fig. 8A and B). Superoxide levels in the lungs were greater in *Idh2*$^{-/-}$ mice than in *Idh2*$^{+/+}$ mice ($p < 0.001$) (Fig. 8E). Mito-TEMPO reduced superoxide levels in both mice ($p = 0.052$ in *Idh2*$^{+/+}$ and $p = 0.001$ in *Idh2*$^{-/-}$). This reduction was greater in *Idh2*$^{-/-}$ mice than in *Idh2*$^{+/+}$ mice (approximately 11.6 % in *Idh2*$^{+/+}$ and 27.2 % in *Idh2*$^{-/-}$) (Fig. 8E). The levels of 4-HNE in BALF increased in both *Idh2*$^{-/-}$ mice and *Idh2*$^{+/+}$ mice, with a greater increase in *Idh2*$^{-/-}$ mice than in *Idh2*$^{+/+}$ mice ($p < 0.001$) (Fig. 8F and G). Mito-TEMPO prevented the increase in 4-HNE expression in both mice (14.9 % in *Idh2*$^{+/+}$ and 45.6 % in *Idh2*$^{-/-}$) (Fig. 8F and G). Next, we determined the levels of Arl13B, ac-α-tubulin, and α-tubulin in BALF. Kidney IR induced increases in Arl13B, ac-α-tubulin, and α-tubulin expression in BALF; these increases were also greater in *Idh2*$^{-/-}$ mice than in *Idh2*$^{+/+}$ mice (Fig. 8H–K). Mito-TEMPO inhibited kidney IR-induced increases in the expression of Arl13B, ac-α-tubulin, and α-tubulin in the BALF, and these inhibitions were also greater in the *Idh2*$^{-/-}$ mice than in the *Idh2*$^{+/+}$ mice (approximately 16.7 % in *Idh2*$^{+/+}$ and 70.4 % in *Idh2*$^{-/-}$ in Arl13B; 33.5 % in *Idh2*$^{+/+}$ and 51.7 % in *Idh2*$^{-/-}$ in ac-α-tubulin; 39.9 % in *Idh2*$^{+/+}$ and 52.5 % in *Idh2*$^{-/-}$ in α-tubulin) (Fig. 8H–K). These results indicate that the deletion of *Idh2* augmented kidney IR-induced lung injury by increasing mitochondrial oxidative stress.

4. Discussion

In the present study, we report that kidney IR-induced lung injury is exacerbated by *Idh2* deletion and that mitochondrial antioxidant treatment attenuates kidney IR-induced lung injury. In addition, kidney IR induces the disruption of cilia in lung cells via oxidative stress, and the resulting disrupted ciliary fragments and proteins are released into BALF. Importantly, this disruption of cilia is prevented by mitochondria-specific antioxidant treatment. In contrast, *Idh2*-deletion exacerbates kidney IR-induced lung cell cilia disruption. These data indicate that kidney IR impairs the redox balance in lung cells in an ischemic-time dependent manner, resulting in oxidative stress of lung tissue and cilia disruption. Moreover, cilia disruption, at least in part, involves AKI-induced lung injury. To the best of our knowledge, this is the first report to demonstrate that AKI causes the disruption of cilia in lung cells by oxidative stress, and the resulting disrupted ciliary fragments and proteins are released into BALF. These results indicate that the prevention of cilia disruption could be a novel strategy for the treatment of AKI-related ALI. Additionally, these data indicate that ciliary proteins and

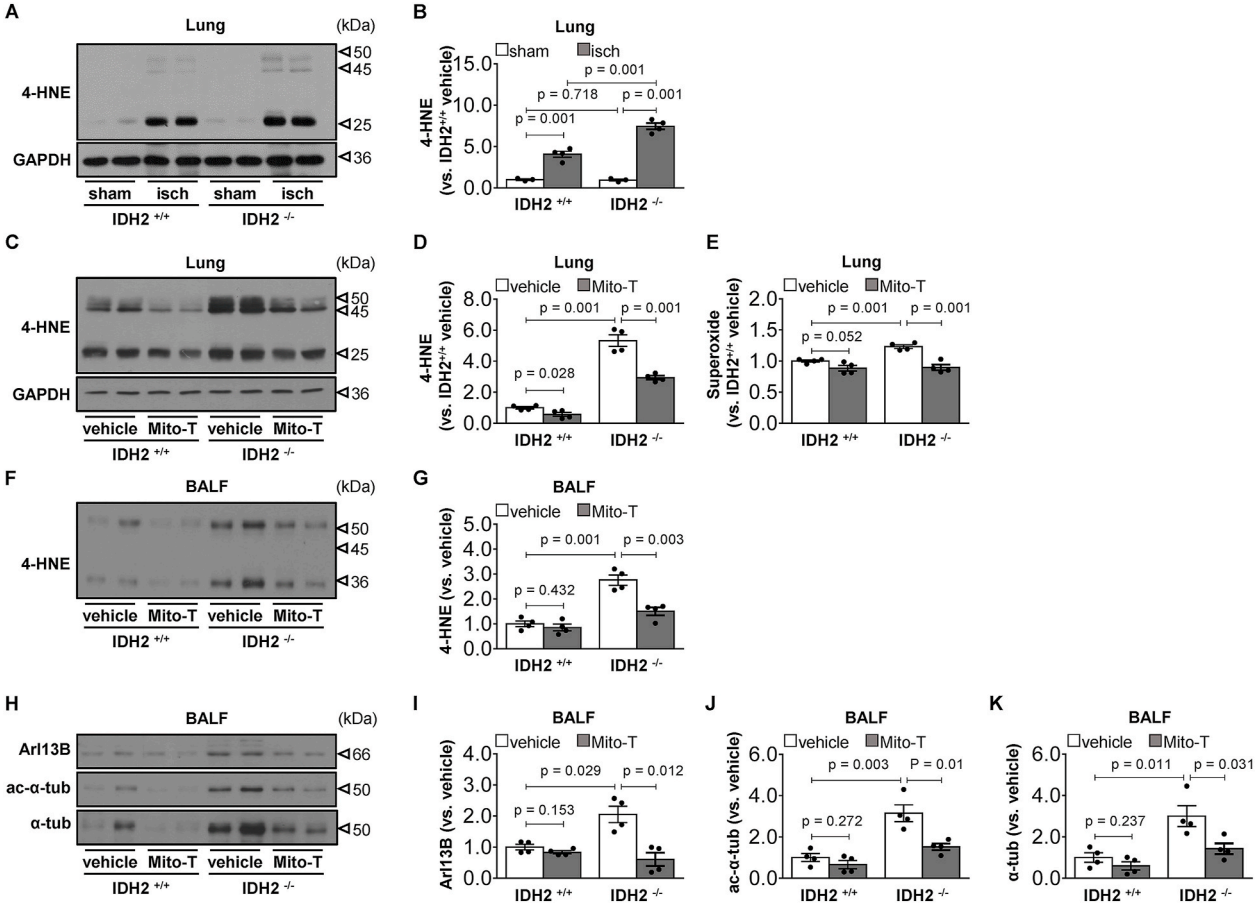

Fig. 8. Greater lung oxidative stress and cilia damage after kidney IR in *Idh2*$^{-/-}$ mice than in *Idh2*$^{+/+}$ mice and greater prevention of stress and damage by Mito-TEMPO in *Idh2*$^{-/-}$ mice than in *Idh2*$^{+/+}$ mice. Female *Idh2*-deleted (*Idh2*$^{-/-}$) and wild-type (*Idh2*$^{+/+}$) littermates were subjected to either 35 min of bilateral renal ischemia (isch) or sham operation. Some mice were administered either Mito-TEMPO (Mito-T, 0.7 mg/kg BW, i.p.) or vehicle 17 and 1 h before ischemia, twice. Lung and BALF were collected 4 h after ischemia. (A-D, F, G) 4-HNE expression in the lung tissues and BALF was evaluated by Western blot analysis (n = 3–4). GAPDH was used as the loading control. The densities of the bands were measured using the ImageJ software. (E) The superoxide level in the lung tissue was measured (n = 4). (F–K) 4-HNE, Arl13B, ac-α-tubulin (ac-α-tub) and α-tubulin (α-tub) expressions in BALF were analyzed by western blotting (n = 4). The densities of bands were measured using the ImageJ software. Results are expressed as the means ± SEM (n = 4).

fragments in BALF could be used an indicator of lung injury.

Kidney IR-induced distant organ injury is a complex process in which numerous factors are involved [4,8,41,42]. Several studies have demonstrated that ROS and oxidative stress contribute to distant organ injury following kidney injury [4,8,41]. In lung injury following kidney IR, it has been proposed that neutrophils, which are infiltrated into the lung, function as major ROS-producing cells in the lung following the stimulation of cytokines produced in injured kidney. This production of ROS subsequently causes additional ROS increases in the lung via the activation of the ROS-producing system and the inhibition of the ROS scavenging system, or both [5,43]. Recently, Hepokoski, M. et al. reported that the extracellular accumulation of kidney mitochondrial DAMPs is caused by AKI, affects lung metabolic pathway, and induces mitochondrial dysfunction [42]. In the present study, we found increased neutrophil infiltration into the lung after kidney IR, depending on kidney ischemic time, i.e., the severity of kidney IR injury. We also found that kidney IR increases superoxide formation, lipid peroxidation, and DNA oxidization in a broad range of lung tissues, including interstitial alveolar septa, alveolar, and airway epithelia. Moreover, we found a decrease in IDH2 expression in the lung tissue after kidney IR. These data indicate that lung cells are exposed to oxidative stress following kidney IR and that this increased oxidative stress, including that by the mitochondria of lung cells, may cause cell and tissue damage and dysfunction. Further, mitochondria-specific antioxidant treatment reduces kidney IR-induced lung injury and inhibits superoxide formation and oxidation of lipids and DNA in lungs.

IDH2 catalyzes the oxidative decarboxylation of isocitrate to α-ketoglutarate in the mitochondria, accompanied by the reduction of NADP to NADPH [31,32,35,44]. NADPH is a source of reducing equivalents for both the thioredoxin and glutathione systems of peroxide detoxification [31,32,35,44,45]. Recently, Park et al. reported that *Idh2* deficiency increases susceptibility to acrolein-induced lung toxicity in Lewis lung carcinoma cells and mice through the disruption of mitochondrial redox balance, leading to mitochondrial oxidative stress and apoptosis [31]. In this study, we found that kidney IR reduced IDH2 expression in the lung and that *Idh2* deletion in mice exacerbated kidney IR-induced lung injury and oxidative stress. In addition, mitochondrial antioxidant supply reduced lung injury and lung oxidative stress with greater reductions in *Idh2*-deleted mice than in wild-type littermates. These data indicate that kidney IR-induced lung injury is associated with reduced IDH2 function and subsequent increase in mitochondrial oxidative stress. Moreover, there may be sex differences in lung injury and lung oxidative stress (note Figs. 1 and 7). However, although we found greater lung injury and oxidative stress and greater protective effect of Mito-TEMPO in *Idh2*-deficient female mice than in wild-type female mice, at similar post-kidney BUN levels (in turn, under similar degree of kidney injury), an association of the severity of kidney injury may not be completely ignored because of the dependency of lung injury on kidney injury. This may be answered by the use of lung-specific antioxidant delivery systems or lung-cell specific conditional knock animals.

The ciliary length in cells is dynamically altered under both physiological and pathophysiological conditions. Recent studies have demonstrated that abnormal alteration of cilia length is associated with the development and progression of various diseases, and cilia is associated with mitochondrial function [17–20,43,46,47]. Under physiological conditions, change in cilia length occurs by either reabsorption or elongation during the normal cell cycle [48–51]. Resorption is a normal process in which cells retract the cilium into the cell during progression from the G0/G1 phase to the S to G2 phases of the cell cycle, and complete cilia reabsorption occurs before mitosis [48–51]. Recent studies have demonstrated that shortening of the cilia length is caused by cell injury [17–20,46,52]. In previous studies, we found that AKI induces the disruption of cilia in kidney tubular epithelial cells as a result of oxidative stress [18–20]. Furthermore, we found that hepatic IR injury induces the deciliation of primary cilia of tubular cells of distant kidneys owing to oxidative stress in kidney tubule cells and that this deciliation is prevented by antioxidant treatment [20]. Moreover, primary cilia deficiency activates the epithelial to mesenchymal transition, which is critical for the progression of fibrosis [53], indicating that cilia are associated with the progression of post-injury responses. In the present study, we found that kidney IR causes the disruption of lung cell cilia, and these disrupted ciliary fragments are released into BALF. In addition, *Idh2* deletion augmented AKI-induced cilia disruption, whereas Mito-TEMPO treatment prevented kidney IR-induced lung cilia damage, with greater preventive effects in $Idh2^{-/-}$ mice than in $Idh2^{+/+}$ mice. Additionally, we found that BALF-containing molecules are highly oxidized and Mito-TEMPO injection reduces the oxidization of BALF contents. Therefore, we speculate that ROS and oxidative stress cause cilia disruption. Supporting this, in previous studies, we found that high concentrations of hydrogen peroxide disrupt cilia in kidney tubule cells [18].

The lung is typically a motile cilia-rich tissue and the dysfunction of respiratory cilia is linked to impaired mucociliary clearance, chest infections, and progressive destruction of lung architecture [54]. In the bronchiole apical region, ciliated cells have abundant mitochondria to produce ATP for the ciliary motion [13]. Studies have reported that mitochondrial damage in ciliated cells causes dysfunction of both cilia and lung cells, which may lead to an abundance of ROS [55,56]. Several studies have reported that impaired mitochondrial dynamics and mitochondrial damage are associated with lung diseases [56,57]. In this present study, we also found that kidney IR causes an abnormal increase in superoxide generation and mitochondrial fission in the lung. In addition, we found increases in ciliary fragments and proteins in BALF of kidney IR mice. Therefore, we speculated that the deciliation is linked, at least in part, to AKI-induced ALI. However, we could not distinguish which types of cilia are disrupted and which cells are major ciliary fragment-releasing cells among lung cells owing to the lack of specific markers of primary and motile cilia and histological study limitations. This limitation may be overcome in additional experiments using lung-specific drug delivery systems or lung-specific ciliary genesis-associated gene targeting. However, our data clearly demonstrate that AKI-related ALI is associated with cilia disruption and oxidative stress of lung cells.

Declaration of competing interest

None.

Acknowledgments

This study was supported by a grant from the National Research Foundation of Korea (NRF) (NRF-2020R1A2C2006903, MIST) funded by the Ministry of Science and ICT (MIST) and a grant from the Korea Health Technology R&D Project (HI15C0001) through the Korea Health Industry Development Institute (KHIDI) funded by the Ministry of Health & Welfare, Korea government.

References

[1] F. Fani, et al., Recent advances in the pathogenetic mechanisms of sepsis-associated acute kidney injury, J. Nephrol. 31 (2018) 351–359.
[2] H.S. Jang, et al., Activation of ERK accelerates repair of renal tubular epithelial cells, whereas it inhibits progression of fibrosis following ischemia/reperfusion injury, Biochim. Biophys. Acta 1832 (2013) 1998–2008.
[3] K.M. Park, A. Chen, J.V. Bonventre, Prevention of kidney ischemia/reperfusion-induced functional injury and JNK, p38, and MAPK kinase activation by remote ischemic pretreatment, J. Biol. Chem. 276 (2001) 11870–11876.
[4] S. Faubel, C.L. Edelstein, Mechanisms and mediators of lung injury after acute kidney injury, Nat. Rev. Nephrol. 12 (2016) 48–60.
[5] S.A. Lee, M. Cozzi, E.L. Bush, H. Rabb, Distant organ dysfunction in acute kidney injury: a review, Am. J. Kidney Dis. 72 (2018) 846–856.
[6] L.E. White, H.T. Hassoun, Inflammatory mechanisms of organ crosstalk during ischemic acute kidney injury, Internet J. Nephrol. 2012 (2012), 505197.

[7] S. Faubel, Acute kidney injury and multiple organ dysfunction syndrome, Minerva Urol. Nefrol. 61 (2009) 171–188.
[8] C.C. Kao, W.S. Yang, J.T. Fang, K.D. Liu, V.C. Wu, Remote organ failure in acute kidney injury, J. Formos. Med. Assoc. 118 (2019) 859–866.
[9] K. Doi, H. Rabb, Impact of acute kidney injury on distant organ function: recent findings and potential therapeutic targets, Kidney Int. 89 (2016) 555–564.
[10] P. Satir, S.T. Christensen, Overview of structure and function of mammalian cilia, Annu. Rev. Physiol. 69 (2007) 377–400.
[11] P. Satir, L.B. Pedersen, S.T. Christensen, The primary cilium at a glance, J. Cell Sci. 123 (2010) 499–503.
[12] H.A. Praetorius, K.R. Spring, A physiological view of the primary cilium, Annu. Rev. Physiol. 67 (2005) 515–529.
[13] X.M. Bustamante-Marin, L.E. Ostrowski, Cilia and mucociliary clearance, Cold Spring Harb Perspect Biol 9 (2017).
[14] S.H. Kathem, A.M. Mohieldin, S.M. Nauli, The roles of primary cilia in polycystic kidney disease, AIMS Mol Sci 1 (2014) 27–46.
[15] L. Eley, L.M. Yates, J.A. Goodship, Cilia and disease, Curr. Opin. Genet. Dev. 15 (2005) 308–314.
[16] B. Thomas, et al., Persistent disruption of ciliated epithelium following paediatric lung transplantation, Eur. Respir. J. 40 (2012) 1245–1252.
[17] K.M. Park, Can tissue cilia lengths and urine cilia proteins Be markers of kidney diseases? Chonnam Med J 54 (2018) 83–89.
[18] J.I. Kim, et al., Reduction of oxidative stress during recovery accelerates normalization of primary cilia length that is altered after ischemic injury in murine kidneys, Am. J. Physiol. Ren. Physiol. 304 (2013) F1283–F1294.
[19] M.J. Kong, et al., Fragmentation of kidney epithelial cell primary cilia occurs by cisplatin and these cilia fragments are excreted into the urine, Redox Biol 20 (2019) 38–45.
[20] S.J. Han, et al., Hepatic ischemia/reperfusion injury disrupts the homeostasis of kidney primary cilia via oxidative stress, Biochim. Biophys. Acta (BBA) - Mol. Basis Dis. 1863 (2017) 1817–1828.
[21] R. Ologunde, H. Zhao, K. Lu, D. Ma, Organ cross talk and remote organ damage following acute kidney injury, Int. Urol. Nephrol. 46 (2014) 2337–2345.
[22] M. Serteser, et al., Changes in hepatic TNF-alpha levels, antioxidant status, and oxidation products after renal ischemia/reperfusion injury in mice, J. Surg. Res. 107 (2002) 234–240.
[23] M.L. Lie, et al., Lung T lymphocyte trafficking and activation during ischemic acute kidney injury, J. Immunol. 189 (2012) 2843–2851.
[24] L.E. White, Y. Cui, C.M. Shelak, M.L. Lie, H.T. Hassoun, Lung endothelial cell apoptosis during ischemic acute kidney injury, Shock 38 (2012) 320–327.
[25] K.J. Kelly, Distant effects of experimental renal ischemia/reperfusion injury, J. Am. Soc. Nephrol. 14 (2003) 1549–1558.
[26] F. Golab, et al., Ischemic and non-ischemic acute kidney injury cause hepatic damage, Kidney Int. 75 (2009) 783–792.
[27] L. Rodriguez-Ribera, C. Slattery, T. Mc Morrow, R. Marcos, S. Pastor, Reactive carbonyl compounds impair wound healing by vimentin collapse and loss of the primary cilium, Food Chem. Toxicol. 108 (2017) 128–138.
[28] S. Kim, et al., Suppression of tumorigenesis in mitochondrial NADP(+)-dependent isocitrate dehydrogenase knock-out mice, Biochim. Biophys. Acta (1842) 135–143, 2014.
[29] C.E. Outten, V.C. Culotta, Alternative start sites in the Saccharomyces cerevisiae GLR1 gene are responsible for mitochondrial and cytosolic isoforms of glutathione reductase, J. Biol. Chem. 279 (2004) 7785–7791.
[30] C.H. Lillig, M.E. Lonn, M. Enoksson, A.P. Fernandes, A. Holmgren, Short interfering RNA-mediated silencing of glutaredoxin 2 increases the sensitivity of HeLa cells toward doxorubicin and phenylarsine oxide, Proc. Natl. Acad. Sci. U. S. A. 101 (2004) 13227–13232.
[31] J.H. Park, H.J. Ku, J.H. Lee, J.W. Park, Idh2 deficiency exacerbates acrolein-induced lung injury through mitochondrial redox environment deterioration, Oxid Med Cell Longev (2017), 1595103 (2017).
[32] S.J. Han, H.S. Choi, J.I. Kim, J.W. Park, K.M. Park, IDH2 deficiency increases the liver susceptibility to ischemia-reperfusion injury via increased mitochondrial oxidative injury, Redox Biol 14 (2018) 142–153.
[33] H.S. Jang, et al., Bone marrow derived cells and reactive oxygen species in hypertrophy of contralateral kidney of transient unilateral renal ischemia-induced mouse, Free Radic. Res. 46 (2012) 903–911.
[34] H.L. Liang, et al., MnTMPyP, a cell-permeant SOD mimetic, reduces oxidative stress and apoptosis following renal ischemia-reperfusion, Am. J. Physiol. Ren. Physiol. 296 (2009) F266–F276.
[35] M.J. Kong, S.J. Han, J.I. Kim, J.W. Park, K.M. Park, Mitochondrial NADP(+)-dependent isocitrate dehydrogenase deficiency increases cisplatin-induced oxidative damage in the kidney tubule cells, Cell Death Dis. 9 (2018) 488.
[36] J. Jezek, K.F. Cooper, R. Strich, Reactive oxygen species and mitochondrial dynamics: the Yin and Yang of mitochondrial dysfunction and cancer progression, Antioxidants 7 (2018).
[37] L. Martinez-Carreres, A. Nasrallah, L. Fajas, Cancer: linking powerhouses to suicidal bags, Front Oncol 7 (2017) 204.
[38] K. Wang, R. Yan, K.F. Cooper, R. Strich, Cyclin C mediates stress-induced mitochondrial fission and apoptosis, Mol. Biol. Cell 26 (2015) 1030–1043.
[39] K.M. Park, J.I. Kim, Y. Ahn, A.J. Bonventre, J.V. Bonventre, Testosterone is responsible for enhanced susceptibility of males to ischemic renal injury, J. Biol. Chem. 279 (2004) 52282–52292.
[40] J. Kim, et al., Orchiectomy attenuates post-ischemic oxidative stress and ischemia/reperfusion injury in mice. A role for manganese superoxide dismutase, J. Biol. Chem. 281 (2006) 20349–20356.
[41] N.M. Abogresha, S.M. Greish, E.Z. Abdelaziz, W.F. Khalil, Remote effect of kidney ischemia-reperfusion injury on pancreas: role of oxidative stress and mitochondrial apoptosis, Arch. Med. Sci. 12 (2016) 252–262.
[42] M. Hepokoski, et al., Altered lung metabolism and mitochondrial DAMPs in lung injury due to acute kidney injury, Am. J. Physiol. Lung Cell Mol. Physiol. 320 (2021) L821–L831.
[43] I. Rahman, I.M. Adcock, Oxidative stress and redox regulation of lung inflammation in COPD, Eur. Respir. J. 28 (2006) 219–242.
[44] S.J. Han, et al., Mitochondrial NADP(+)-Dependent isocitrate dehydrogenase deficiency exacerbates mitochondrial and cell damage after kidney ischemia-reperfusion injury, J. Am. Soc. Nephrol. 28 (2017) 1200–1215.
[45] H. Nakamura, Thioredoxin and its related molecules: update 2005, Antioxidants Redox Signal. 7 (2005) 823–828.
[46] S. Wang, Z. Dong, Primary cilia and kidney injury: current research status and future perspectives, Am. J. Physiol. Ren. Physiol. 305 (2013) F1085–F1098.
[47] M.D. Burkhalter, et al., Imbalanced mitochondrial function provokes heterotaxy via aberrant ciliogenesis, J. Clin. Invest. 129 (2019) 2841–2855.
[48] L.M. Quarmby, Cellular deflagellation, Int. Rev. Cytol. 233 (2004) 47–91.
[49] L.M. Quarmby, J.D. Parker, Cilia and the cell cycle? J. Cell Biol. 169 (2005) 707–710.
[50] C.H. Sung, A. Li, Ciliary resorption modulates G1 length and cell cycle progression, Cell Cycle 10 (2011) 2825–2826.
[51] C.E. Overgaard, et al., Deciliation is associated with dramatic remodeling of epithelial cell junctions and surface domains, Mol. Biol. Cell 20 (2009) 102–113.
[52] E. Verghese, et al., Renal primary cilia lengthen after acute tubular necrosis, J. Am. Soc. Nephrol. 20 (2009) 2147–2153.
[53] S.J. Han, et al., Deficiency of primary cilia in kidney epithelial cells induces epithelial to mesenchymal transition, Biochem. Biophys. Res. Commun. 496 (2018) 450–454.
[54] A.E. Tilley, M.S. Walters, R. Shaykhiev, R.G. Crystal, Cilia dysfunction in lung disease, Annu. Rev. Physiol. 77 (2015) 379–406.
[55] S.M. Cloonan, A.M. Choi, Mitochondria in lung disease, J. Clin. Invest. 126 (2016) 809–820.
[56] M. Aghapour, et al., Mitochondria: at the crossroads of regulating lung epithelial cell function in chronic obstructive pulmonary disease, Am. J. Physiol. Lung Cell Mol. Physiol. 318 (2020) L149–L164.
[57] B. Kosmider, et al., Mitochondrial dysfunction in human primary alveolar type II cells in emphysema, EBioMedicine 46 (2019) 305–316.